

Catalysis Science & Technology

Accepted Manuscript



This is an *Accepted Manuscript*, which has been through the Royal Society of Chemistry peer review process and has been accepted for publication.

Accepted Manuscripts are published online shortly after acceptance, before technical editing, formatting and proof reading. Using this free service, authors can make their results available to the community, in citable form, before we publish the edited article. We will replace this *Accepted Manuscript* with the edited and formatted *Advance Article* as soon as it is available.

You can find more information about *Accepted Manuscripts* in the [Information for Authors](#).

Please note that technical editing may introduce minor changes to the text and/or graphics, which may alter content. The journal's standard [Terms & Conditions](#) and the [Ethical guidelines](#) still apply. In no event shall the Royal Society of Chemistry be held responsible for any errors or omissions in this *Accepted Manuscript* or any consequences arising from the use of any information it contains.

ARTICLE

Tuning the Chemoselective Hydrogenation of Aromatic Ketones, Aromatic Aldehydes and Quinolines Catalyzed by Phosphine Functionalized Ionic Liquids Stabilized Ruthenium Nanoparticles

Cite this: DOI: 10.1039/x0xx00000x

Received 00th January 2012,
Accepted 00th January 2012

DOI: 10.1039/x0xx00000x

www.rsc.org/

He-yan Jiang*^a and Xu-xu Zheng^a

Ruthenium nanoparticles (Ru NPs) stabilized by phosphine-functionalized ionic liquids (PFILs) were synthesized in imidazolium based ionic liquid using H₂ as a reductant. Characterization showed well-dispersed particles of about 2.2 nm (TEM) and confirmed the PFIL stabilization of the Ru NPs (NMR). The Ru NPs stabilized by PFILs exhibited excellent activity and switchable chemoselectivity in the heterogeneous selective hydrogenation of aromatic ketones, aromatic aldehydes and quinolines under mild conditions.

Introduction

Metal nanoparticles are fascinating because of their applications in such areas as optoelectronics, sensing, medicine as well as in catalysis.¹⁻⁵ The investigation of metal nanoparticles in catalysis has been receiving increasing interest because nanometal particles present an efficient combination of the advantages of heterogeneous and homogeneous catalysts. Additional stabilization, generally provided by phosphines, amines or polymers, of nanoparticles influences the catalytic activity, selectivity and recyclability.⁶⁻¹² Ionic liquid stabilized metal nanoparticles are interesting new catalytic materials for hydrogenation and other applications.³ Furthermore, with both a covalent and an electrostatic stabilization, functionalized ionic liquids containing metalbinding moieties have been gradually employed in the synthesis of transition metal nanoparticles to improve catalytic system stability and/or catalytic performance.¹³⁻¹⁷ However, up to now, ionic liquid stabilized metal nanoparticles were tested as catalysts mainly in the hydrogenation of alkenes or arenes.^{3,18-21}

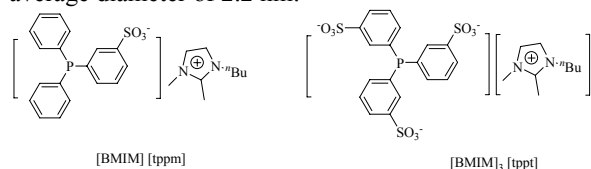
The chemoselective reduction of aromatic compounds (aromatic ketones, aromatic aldehydes, quinolines etc.) by means of heterogeneous catalysis is an important field in industrial hydrogenation process.²²⁻³¹ Furthermore, tuning the hydrogenation chemoselectivity of aromatic compounds on heterogeneous catalysis remains a formidable scientific challenge. We focus on the selective hydrogenation of aromatic compounds, an important organic transformation, since the resulting products are versatile precursors to many natural products and drug molecules. As part of our ongoing research,³²⁻³⁴ we herein disclose a practical, general, and efficient method that aromatic compounds can be hydrogenated with switchable excellent chemoselectivity under mild conditions catalyzed by ruthenium nanoparticles (Ru NPs) stabilized by phosphine-functionalized ionic liquids (PFILs). To the best of our knowledge, the approach used here has not been explored before.

Results and Discussion

Synthesis and Characterization of Ruthenium Nanoparticles

The synthesis of Ru NPs was achieved through the reduction of RuO₂·xH₂O or Ru(COD)(2-methylallyl)₂ (COD=cycloocta-1,5-diene) in [BMIM]BF₄ (BMIM=1-butyl-2,3-dimethylimidazolium) under an atmosphere of H₂ (1 MPa) in the presence of 1.0 equivalent of PFILs [BMIM][tppm] or [BMIM][tppt] (Fig. 1), which afforded a dark suspension. For comparison, Ru NPs were also synthesized in [BMIM]BF₄ in the absence of any additional stabilizer. A black powder could be isolated from the black suspension by adding acetone and then centrifuging (8000 rpm for 10 min). Washed three times with acetone and dried under reduced pressure, the isolated powder was analyzed by transmission electron microscopy (TEM), X-ray photoelectron spectroscopy (XPS), X-ray diffraction (XRD), nuclear magnetic resonance (NMR) and infrared spectroscopy (IR).

TEM analysis was employed to characterize the isolated Ru NPs and determine their mean diameter (Fig. 2). In general, Ru NPs prepared from precursor RuO₂·xH₂O showed better dispersion than from [Ru(COD)(2-methylallyl)₂] (Fig. 2, images 1, 2 *versus* 3, 4), and the TEM image showed a trend toward agglomeration of the Ru NPs in the absence of functionalized ionic liquid (Fig. 2, image 5). The TEM image of isolated Ru NPs **1**, derived from RuO₂·xH₂O, showed the formation of nearly monodispersed Ru nanoparticles with an average diameter of 2.2 nm.



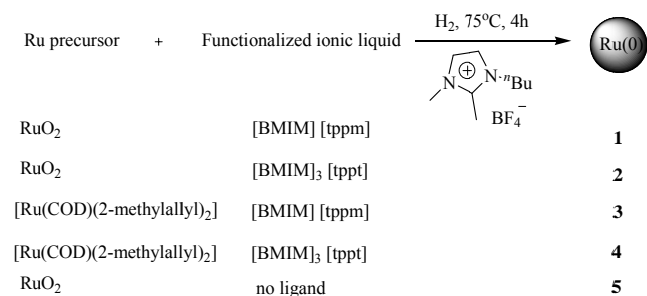


Fig. 1 Synthesis of Ru NPs in [BMIM]BF₄

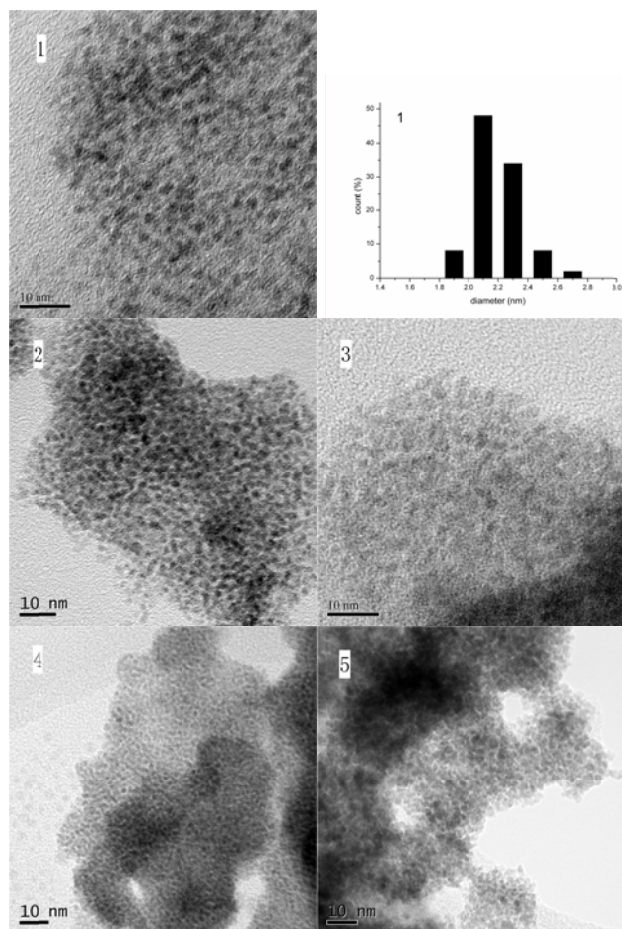


Fig. 2 TEM images of Ru nanoparticles 1, 2, 3, 4 and 5

The XPS analysis of the isolated Ru NPs **1** was employed to elucidate the nature of the stabilizing layer of the nanometal particles. XPS analysis of Ru NPs stabilized by [BMIM][tppm] showed the presence of ruthenium, phosphorus, nitrogen and carbon, which signified the presence of [BMIM][tppm] in the ligand sphere of the Ru NPs. The X-ray diffraction pattern of isolated Ru NPs **1** (Fig. 3) generally showed the predicted lines of the Ru hcp structure in the wide-angle range.

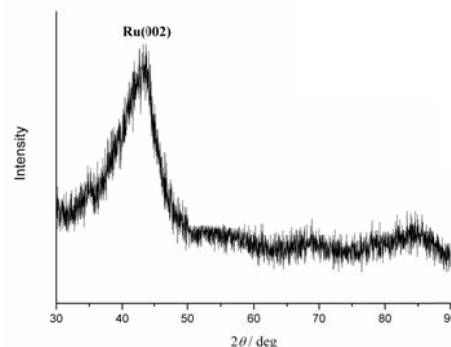


Fig. 3 X-Ray diffraction pattern of isolated Ru NPs **1**

³¹P NMR studies of [BMIM][tppm] and [BMIM][tppm] stabilized Ru NPs **1** in [BMIM]BF₄ were conducted. The ³¹P NMR spectrum of [BMIM][tppm] was $\delta = -5.4$ ppm. However, no signal was detected in the ³¹P NMR spectrum of Ru NPs **1**. Further stirred the mixture of isolated Ru NPs **1** and hydrogen peroxide at 50 °C for 10 h, a oxide signal of [BMIM][tppm] appeared at $\delta = 30.0$ ppm. The ³¹P NMR observations may be explained that majority of the [BMIM][tppm] were attached to Ru NPs surface, and free phosphine and attached phosphine exchange very fast affording no ³¹P NMR signal.

IR is effective for the investigation of the mutual ligand-metal interactions of nanometal catalysts. Information on the interaction between the nanometal and the phosphine in Ru NPs **1** was confirmed by FTIR methods in which the red shift of the P-C₆H₅ deformation around 1469 cm⁻¹ in Ru NPs **1** is an indication of the coordination of [BMIM][tppm] to the metal Ru(0).

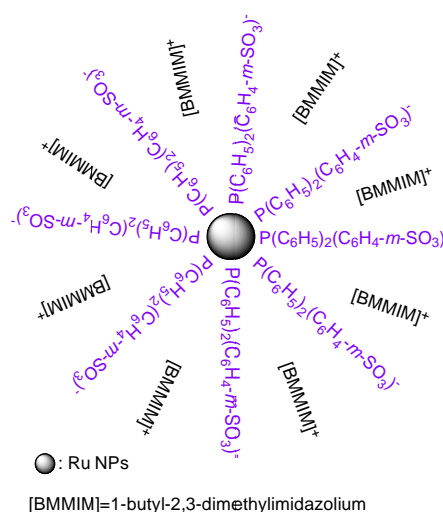


Fig. 4 The PFIL ([BMIM][tppm]) stabilized/modified Ru nanoparticles

The effect of [BMIM][tppm] in catalyst is noteworthy. Due to the strong coordination capacity of the anion of [BMIM][tppm], Ru NPs were well dispersed and highly stable in catalytic hydrogenation. On the basis of these results, it was deduced that the $[\text{P}(\text{C}_6\text{H}_5)_2(\text{C}_6\text{H}_4\text{-}m\text{-SO}_3)]^-$ ions formed a layer around the surface of the Ru NPs, leading to a sphere of negative charge, and then the cation of [BMIM][tppm] became arranged as an outer layer for charge conservation (Fig. 4).

Recently, several groups have demonstrated ionic liquids possess self-organized structures, which can create an external layer around the surface of the metal NPs to protect them from aggregation^{5,20,35}.

Catalytic hydrogenation

Initially, we chose styrene as a model substrate to explore the catalytic performance of Ru NPs **1** under very mild conditions (30 °C, H₂ at 1MPa). Fig. 5 shows the effect of the conversion versus time. The hydrogenation of styrene produced only ethylbenzene in the test. It was found that the conversion increased linearly with time, showing no induction period, proving that this catalyst did not convert into other catalytically active species. Furthermore, mercury-poisoning experiments were run as they can selectively poison metal nanoparticles, by forming an amalgam with mercury, to help distinguish between homogeneous and heterogeneous catalysts.³⁶ In such an experiment, the conversion was 61.6 % after the initial 1 hour; mercury was then added under argon atmosphere and the reaction was completely terminated as evidenced by no change in the conversion after an additional reaction time of 3 hours. In addition, it was found that the amount of leaching from Ru NPs **1** was about 0.9 ppm by ICP-AES analysis of the organic phase in styrene catalytic hydrogenation. The catalyst could be reused by simple liquid-liquid extraction after reaction. The procedure was repeated ten times and the results indicated that Ru NPs **1** could be recycled without any loss of catalytic activity (Fig. 6). The average diameter of the spent Ru NPs **1** after ten recycles of styrene hydrogenation was 2.13 nm (S2 and S3 in ESI). All the results above strongly supported proposal that the reaction progressed under heterogeneous catalysis rather than homogeneous catalysis.

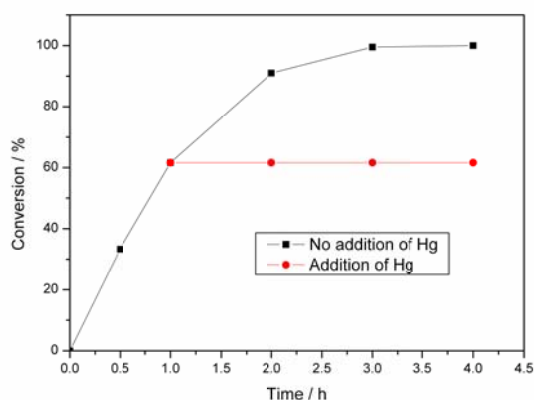


Fig. 5 Reaction profiles for hydrogenation of styrene and Hg⁰ poisoning of the Ru NPs **1**. Reaction conditions: styrene (8.9×10^{-3} mol; styrene/Ru=500), 30 °C, H₂ at 1MPa.

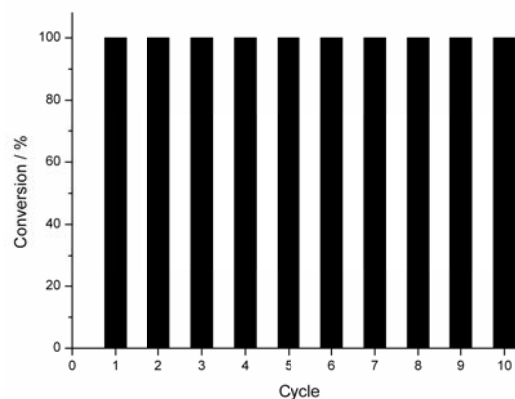
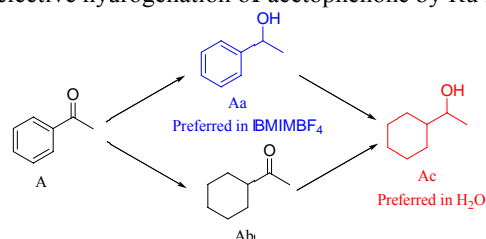


Fig. 6 Recyclability of Ru NPs **1** for the hydrogenation of styrene. Reaction conditions: styrene (8.9×10^{-3} mol; styrene/Ru=500), 30 °C, H₂ at 1MPa.

The chemoselective reduction of carbonyl compounds by means of heterogeneous catalysis is of considerable importance in the synthesis of fine chemicals, particularly intermediates in the fragrance and pharmaceutical industries.²²⁻²⁵ Baiker and coworkers found that Pd-[BMIm][PF₆] exhibited good activity and selectivity in the hydrogenation of acetophenone.²³ However, tuning the hydrogenation chemoselectivity of aromatic carbonyl compounds on heterogeneous catalysis remains rather difficult. The effect of different reaction factors on the chemoselective hydrogenation of acetophenone is listed in Table 1. The importance of basic additive in a catalyst system for the selective hydrogenation of aromatic ketones has been well-established.^{37,38} The Ru NPs had no catalytic activity under ambient temperature in [BMIM]BF₄ in the absence of basic additive (Table 1, entry 1). Similar to the previous reports, a basic additive was helpful to improve the catalytic performance, acetophenone could be hydrogenated with 77.0% conversion and 99.0% chemoselectivity to 1-phenylethanol in the presence of [BMIM]OH (1-butyl-2,3-dimethylimidazolium hydroxide) (Table 1, entry 2). The PFIL stabilizers showed important influence on the catalytic process; without the stabilizer, the hydrogenation resulted in a conversion of 94% and a chemoselectivity as low as 76.6% to 1-phenylethanol (Table 1, entry 4). Ru NPs stabilized by [BMIM][tppm] showed lower activity but higher chemoselectivity to 1-phenylethanol than Ru NPs stabilized by [BMIM][tppt] (Table 1, entries 2-3). These results indicated that PFILs not only stabilized the metal particles in the preparation of the catalyst, but also served to additionally modify the Ru NPs in the chemoselective hydrogenation.

Table 1. Optimization of reaction conditions for the chemoselective hydrogenation of acetophenone by Ru NPs. ^a



Entry	Catalyst	Solvent	t (h)	Conversion (%)	Selectivity (%)		
					Aa	Ab	Ac
1	1	BMIMBF ₄	15	0.0	-	-	-
2	1 ^b	BMIMBF ₄	15	77.0	99.0	0.4	0.6
3	2 ^b	BMIMBF ₄	15	92.0	84.0	6.2	9.8
4	5 ^b	BMIMBF ₄	15	94.0	76.6	3.4	20.0
5	3 ^b	BMIMBF ₄	15	48.0	94.2	2.9	2.9
6	4 ^b	BMIMBF ₄	15	69.0	92.6	2.7	4.7
7	Ru/C ^b	BMIMBF ₄	15	0.0	-	-	-
8	1 ^c	H ₂ O	1	100.0	0.0	0.4	99.6
9	5 ^c	H ₂ O	1	26.1	55.9	18.4	25.7
10	Ru/C	H ₂ O	1	99.0	34.6	1.2	64.2

^a Reaction was carried out at 30°C. Substrate: in a 1 ml solution at [1.8M], PH₂:5.0MPa. Substrate/Ru=100:1, Ru/C (5 wt%, 36 mg). Products were analyzed by a GC instrument with an FID detector and β-DEX120 capillary column. ^b [BMIM]OH=0.20 molL⁻¹ was added. ^c Ru nanoparticles were isolated and redispersed in water.

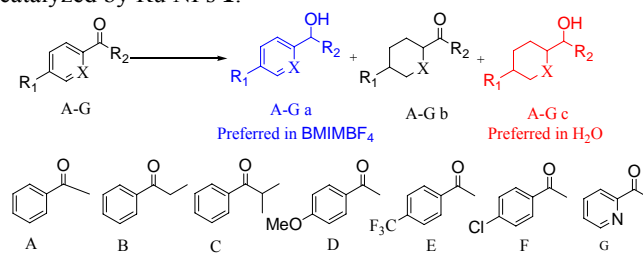
Since the properties of the metal precursors greatly influence the particle size and dispersion of nanometal catalysts.^{3,4} Metal precursors, including RuO₂·xH₂O and [Ru(COD)(2-methylallyl)₂], were tested. Generally, Ru NPs **1** and **2**, prepared from RuO₂·xH₂O, showed higher activity than **3** and **4**, which were prepared from [Ru(COD)(2-methylallyl)₂] (Table 1, entries 2-3 *versus* 5-6). The best chemoselectivity of 99.0% was achieved in the hydrogenation of acetophenone to 1-phenylethanol using Ru NPs **1** as the catalyst.

The best solvent is no solvent and if a solvent is needed then water is preferred.³⁹ Indeed, water is an attractive alternative to traditional organic solvents because it is cheap, readily available, nontoxic, non-flammable and safe to environment. Ru NPs **1** isolated from centrifugation was redispersed in water to test the catalytic performance (Table 1, entry 8). To our surprise, when water was used as the solvent in the hydrogenation of acetophenone, the reaction progressed very fast with a high chemoselectivity to cyclohexylethanol. In comparison with catalytic hydrogenation in ionic liquid BMIMBF₄, the high catalytic activity in water may be attributed to the increased substrate solubility in water as well as the interactions between water and substrate *via* hydrogen bonding.⁴⁰ However, Ru NPs **5** isolated from centrifugation and redispersed in water showed poor activity and chemoselectivity (Table 1, entry 9).

Commercially available Ru/C catalyst was also tested under similar reaction conditions in the hydrogenation of acetophenone (Table 1, entries 7 and 10). Overall, Ru/C catalyst showed poor activity and chemoselectivity towards either 1-phenylethanol or cyclohexylethanol.

Some representative examples are listed in Table 2 for the chemoselective hydrogenation of aromatic ketones catalyzed by Ru NPs **1** in both [BMIM]BF₄ and water. The extent of the chemoselectivity appears to be delicately influenced by the substituent in the substrate. In general, the activity and chemoselectivity decreased by increasing the bulkiness of the alkyl group from methyl or primary alkyl to isopropyl (Table 2, entries 1-6). It was found that when the substituent is in the *para* position, substrate with electron-donating group showed poor reaction activity with excellent chemoselectivity to C=O hydrogenation product in [BMIM]BF₄ or full hydrogenation product in water (Table 2, entries 7-8), and substrates with electron-drawing groups showed good reaction activity with the major chemoselectivity to C=O hydrogenation products in both [BMIM]BF₄ and water (Table 2, entries 9-12). Furthermore, 2-acetothiophene, 2-acetopyridine, and 2-acetopyrrole were also tested, 2-acetothiophene and 2-acetopyrrole showed no reaction activity during the test. The chemoselectivity of 2-acetopyridine to C=O and full hydrogenation products could reach 96.7% and 100% respectively (Table 2, entries 13-14). The effect of the steric bulk and the electronic nature of the substrates influence the activity and the chemoselectivity of the reaction.

Table 2. Chemoselective hydrogenation of aromatic ketones catalyzed by Ru NPs **1**.^a



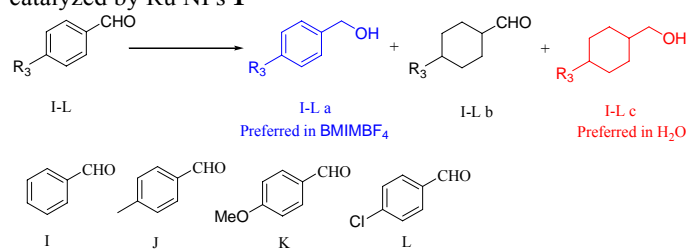
Entry	A-G	Solvent	t (h)	Conversion (%)	Selectivity (%)		
					A-G a	A-G b	A-G c
1	A	BMIMBF ₄	15	77.0	99.0	0.4	0.6
2 ^b	A	H ₂ O	1	100.0	0.0	0.4	99.6
3	B	BMIMBF ₄	15	21.0	86.0	14.0	0.0
4 ^b	B	H ₂ O	2	100.0	0.0	4.5	95.5
5	C	BMIMBF ₄	15	10.4	80.0	20.0	0.0
6 ^b	C	H ₂ O	2	72.5	21.0	38.0	41.0
7	D	BMIMBF ₄	15	2.0	100.0	0.0	0.0
8 ^b	D	H ₂ O	2	99.0	0.0	0.0	100.0
9	E	BMIMBF ₄	15	100.0	100.0	0.0	0.0
10 ^b	E	H ₂ O	2	100.0	92.1	3.3	4.6
11	F	BMIMBF ₄	15	72.0	85.0	9.7	5.3

12 ^b	F	H ₂ O	2	59.3	93.3	0.3	6.4
13	G	BMIMBF ₄	15	26.4	96.7	0.0	3.3
14 ^b	G	H ₂ O	2	100.0	0.0	0.0	100.0

^a The reaction conditions are the same as in Table 1. When BMIMBF₄ was the solvent, [BMIM]OH=0.20 molL⁻¹ was added. ^b Ru nanoparticles **1** were isolated and redispersed in water.

The chemoselective hydrogenation of aromatic aldehydes were also tested (Table 3). In comparison to the chemoselective hydrogenation of aromatic ketones, aromatic aldehydes could be hydrogenated to corresponding C=O and full hydrogenation products easily. Without the basic additive, benzaldehyde could be hydrogenated to corresponding benzyl alcohol in [BMIM]BF₄ (Table 3, entry 1). Complete hydrogenation product of benzaldehyde could be achieved in water (Table 3, entry 2). When the substituent is in the *para* position of benzaldehyde, C=O and full hydrogenation could be achieved in weak electron-donating group and electron-drawing group substituted substrates (Table 3, entries 3-5 and 9-11). With strong electron-donating group in the *para* position, *p*-anisaldehyde could be hydrogenated with the major chemoselectivity to C=O hydrogenation product during our test (Table 3, entries 6-8).

Table 3. Chemoselective hydrogenation of aromatic aldehydes catalyzed by Ru NPs **1**^a



Entry	I-L	Solvent	t (h)	Conversion (%)	Selectivity (%)		
					I-L a	I-L b	I-L c
1	I	BMIMBF ₄	15	100.0	100.0	0.0	0.0
2 ^b	I	H ₂ O	1	100.0	0.0	0.0	100.0
3	J	BMIMBF ₄	15	30.5	100.0	0.0	0.0
4 ^b	J	H ₂ O	1	94.7	96.6	0.0	3.4
5 ^b	J	H ₂ O	3	100.0	0.5	0.0	99.5
6	K	BMIMBF ₄	15	0.0	-	-	-
7 ^b	K	H ₂ O	1	99.8	97.0	0.0	3.0
8 ^b	K	H ₂ O	3	100.0	87.9	0.0	12.1

9	L	BMIMBF ₄	15	97.2	100.0	0.0	0.0
10 ^b	L	H ₂ O	1	97.8	0.1	0.0	99.9
11 ^b	L	H ₂ O	3	100.0	0.0	0.0	100.0

^a Reaction was carried out at 30°C. Substrate: in a 1 ml solution at [1.8M], PH₂:3.0MPa. Substrate/Ru=100:1. Products were analyzed by a GC instrument with an FID detector and β-DEX120 capillary column. ^b Ru nanoparticles **1** were isolated and redispersed in water.

Hydrogenation of quinoline and its derivatives is of considerable industrial interests for the production of petrochemicals, fine chemicals, and pharmaceuticals.²⁶⁻²⁸ However, tuning the hydrogenation chemoselectivity of quinolines on heterogeneous catalysis under mild conditions remains a formidable scientific challenge. We investigated the catalytic performance of Ru NPs for the hydrogenation of quinoline and its derivatives (Table 4). Quinoline could be easily hydrogenated to 1,2,3,4-tetrahydroquinoline at 50 °C with 98.0% chemoselectivity in [BMIM]BF₄ and 99.0% chemoselectivity in water (Table 4, entries 1-2). Unprecedentedly, complete hydrogenation of quinoline could also be achieved with 98.2% chemoselectivity in water at a reaction temperature as low as 60 °C (Table 4, entry 3). Commercially available Ru/C catalyst was also tested under similar reaction conditions in the hydrogenation of quinoline (Table 4, entries 4-6). Ru/C catalyst showed poor activity with the major chemoselectivity to 1,2,3,4-tetrahydroquinoline during the test. Quinoline analogues were also tested. Generally, the hydrogenation activity of 2- or 3-methylquinoline was almost the same with quinoline. The presence of substituent in 2-position of quinoline would cause the decrease of the hydrogenation chemoselectivity due to the steric hindrance. Introducing a methyl group in quinoline molecule, especially in 3-position of quinoline, obviously promoted the formation of decahydroquinoline (Table 4, entry 12). 8-methylquinoline could be hydrogenated with absolute chemoselectivity to 1,2,3,4-tetrahydroquinoline during the test (Table 4, entries 13-15).

Table 4. Chemoselective hydrogenation of quinoline and derivatives catalyzed by Ru NPs **1**^a

Entry	Catalyst	M-P	Solvent	T (°C)	Conversion (%)	Selectivity (%)		
						M-P a	M-P b	M-P c
1	1	M	BMIMBF ₄	50	95.0	98.0	2.0	0.0
2	1 ^{b,c}	M	H ₂ O	50	93.0	99.0	0.3	0.7
3	1 ^c	M	H ₂ O	60	98.6	1.8	0.0	98.2
4	Ru/C	M	BMIMBF ₄	50	67.0	98.0	2.0	0.0
5	Ru/C ^b	M	H ₂ O	50	30.0	98.6	0.0	1.4

6	Ru/C	M	H ₂ O	60	92.0	75.9	22.5	1.6
7	1	N	BMIMBF ₄	50	98.4	96.0	4.0	0.0
8	1 ^{bc}	N	H ₂ O	50	81.3	55.5	44.5	0.0
9	1 ^c	N	H ₂ O	60	97.7	1.3	30.4	68.3
10	1	O	BMIMBF ₄	50	97.9	87.7	0.0	12.3
11	1 ^{bc}	O	H ₂ O	50	86.8	24.4	0.0	75.6
12	1 ^c	O	H ₂ O	60	100.0	0.0	0.0	100.0
13	1	P	BMIMBF ₄	50	46.0	100.0	0.0	0.0
14	1 ^{bc}	P	H ₂ O	50	71.7	100.0	0.0	0.0
15	1 ^c	P	H ₂ O	60	95.8	100.0	0.0	0.0

^a Reaction conditions: substrate in a 1 ml solution at [1.8M], PH₂:5.0MPa. Substrate/Ru=100:1, Ru/C (5 wt%, 36 mg). Products were analyzed by a GC instrument with an FID detector and HP-5 column, reaction time: 15 h. ^b Reaction time: 1 h. ^c Ru nanoparticles **1** were isolated and redispersed in water.

Conclusions

The results of this study demonstrated that PFILs stabilized Ru NPs are effective catalysts for the challenging selective hydrogenation of aromatic ketones, aromatic aldehydes and quinolines with a distinct high and switchable selectivity towards different functional groups of substrates. The catalytic performance is complementary to both classical homogeneous and heterogeneous catalysis. Additional work is currently in progress in this and related areas.

Experimental Section

Materials

All manipulations involving air-sensitive materials were carried out using standard Schlenk line techniques under an atmosphere of nitrogen. RuO₂·xH₂O, Ru(COD)(2-methylallyl)₂ and Ru/C (5%) were purchased from Acros. Various substrates and other reagents were analytical grade. The purity of hydrogen was over 99.99%. Phosphine-functionalized ionic liquids were synthesized according to literature.^{41,42} Products were analyzed by GC instrument (cyclohexylcyclohexane used as an internal standard) with an FID detector and HP-5 column (30 m × 0.25 mm) / β-DEX120 capillary column (25 m × 0.25 mm). Products were confirmed by GC-MS and NMR. The TEM analyses were performed in a JEOL JEM 2010 transmission electron microscope operating at 200 kV with nominal resolution of 0.25 nm. The X-ray photoelectron spectroscopy (XPS) measurements were performed on a Thermo ESCALAB 250 spectrometer. The XRD analysis was performed in a D/MAX 2550 VB/PC using a graphite crystal as monochromator. Ru and P contents were characterized by Perkin Elmer Optima 2100DV ICP-AES (S1 in ESI).

Synthesis of ruthenium nanoparticles

Preparation of nanocatalysts 1, 2 or 5: In a typical experiment, RuO₂·xH₂O (0.018 mmol) and PFILs (0.018 mmol for **1** and **2**, no ligand for **5**) were dispersed in [BMIM]BF₄ (1 mL) (BMIM=1-butyl-2,3-dimethylimidazolium) and the reaction mixture was placed in a 20 mL stainless-steel high pressure reactor. After stirring the mixture at room temperature under an atmosphere of N₂ for 30 min, a constant pressure of H₂ (1 MPa) was admitted to the system and the content was stirred for 4 h at 75 °C. The reactor was cooled to ambient temperature and carefully vented. A dark solution was obtained. The Ru NPs embedded in [BMIM]BF₄ were employed for

hydrogenation studies (see below). Isolation of the Ru NPs for TEM, XPS, XRD analysis and for catalytic experiments (see below) was achieved by dissolving the mixture in acetone (5 mL), centrifuging (8000 rpm for 10 min), washing with acetone (2 × 5 mL) and drying under vacuum. Furthermore, the supernatant of the [BMIM][tppm]-stabilized Ru NPs **1** was analyzed by ICP-AES methods and about 2.2% Ru and 5.4% [BMIM][tppm] were lost during the washing and drying procedure.

Preparation of nanocatalysts 3 or 4: In a typical experiment, Ru(COD)(2-methylallyl)₂ (0.018 mmol) and PFILs (0.018 mmol) were dispersed in [BMIM]BF₄ (1 mL) and the reaction mixture was placed in a 20 mL stainless-steel high pressure reactor. After stirring the mixture at room temperature under an atmosphere of N₂ for 30 min, a constant pressure of H₂ (1 MPa) was admitted to the system and the content was stirred for 4 h at 75 °C. The reactor was cooled to ambient temperature and carefully vented. A dark brown solution was obtained that was used for the hydrogenation reaction (see below). Isolation of the Ru NPs for TEM analysis and catalytic experiments (see below) was achieved by dissolving the mixture in acetone (5 mL), centrifuging (8000 rpm for 10 min), washing with acetone (2 × 5 mL) and drying under vacuum.

General procedure for the heterogeneous chemoselective hydrogenation

In [BMIM]BF₄: The stainless steel autoclave containing previously prepared PFIL-stabilized Ru(0) catalyst was charged with the appropriate substrate, then the autoclave was sealed and purged with pure hydrogen several times. After the reactants were heated to predetermined temperature, the reaction timing began. After completion of the reaction and cooling to ambient temperature, the products were isolated by liquid-liquid extraction with diethyl ether and analyzed by gas chromatography.

In water: The isolated nanoparticles dispersed in water (1ml) were placed in a stainless steel autoclave, and the substrate was added. Then the autoclave was sealed and purged with pure hydrogen several times. After the reactants were heated to predetermined temperature, the reaction timing began. After completion of the reaction and cooling to ambient temperature, the products were isolated by liquid-liquid extraction with diethyl ether or centrifugation and analyzed by gas chromatography.

Acknowledgements

This work was financially supported by National Natural Science Foundation of China (No. 21201184), Natural Science Foundation Project of CQ (No. cstc2014jcyjA10105), Ministry of Education of Chongqing (No. KJ1400601), Chongqing Key Laboratory of Catalysis and Functional Organic Molecules (No. 1456028) and 100 leading scientists promotion project of Chongqing.

Notes and references

^a Key Laboratory of Catalysis Science and Technology of Chongqing Education Commission, Chongqing Key Laboratory of Catalysis and Functional Organic Molecules, Chongqing Technology and Business University, Chongqing 400067, P.R. China. E-mail: orgjiang@163.com; Tel./fax: +86 23 6276 9652.

1 K. J. Klabunde and R. M. Richards, *Nanoscale Materials in Chemistry*, Wiley-Interscience, New York, 2001.

- 2 G. Schmid, *Clusters and Colloids. From Theory to Applications*, Wiley VCH, Weinheim, 2004.
- 3 J. Dupont and J. D. Scholten, *Chem. Soc. Rev.*, 2010, **39**, 1780-1804.
- 4 Y. Yuan, N. Yan and P. J. Dyson, *ACS Catal.*, 2012, **2**, 1057-1069.
- 5 K. L. Luska and A. Moores, *ChemCatChem*, 2012, **4**, 1534-1546.
- 6 Y. M. A. Yamada, T. Arakawa, H. Hocke and Y. Uozumi, *Angew. Chem., Int. Ed.*, 2007, **46**, 704-706.
- 7 D. Astruc, F. Lu and J. R. Aranzues, *Angew. Chem., Int. Ed.*, 2005, **44**, 7852-7872.
- 8 S. Jansat, M. Gomez, K. Philippot, G. Muller, E. Guiu, C. Claver, S. Castillon and B. Chaudret, *J. Am. Chem. Soc.*, 2004, **126**, 1592-1593.
- 9 H. Mao, J. Ma, Y. Liao, S. Zhao and X. Liao, *Catal. Sci. Technol.*, 2013, **3**, 1612-1617.
- 10 G. S. Fonseca, A. P. Umpierre, P. F. P. Fichtner, S. R. Teixeira and J. Dupont, *Chem. Eur. J.*, 2003, **9**, 3263-3269.
- 11 C. Vollmer, E. Redel, K. Abu-Shandi, R. Thomann, H. Manyar, C. Hardacre and C. Janiak, *Chem. Eur. J.*, 2010, **16**, 3849-3858.
- 12 P. S. Roy and S. K. Bhattacharya, *Catal. Sci. Technol.*, 2013, **3**, 1314-1323.
- 13 R. R. Dykeman, N. Yan, R. Scopelliti and P. J. Dyson, *Inorg. Chem.*, 2011, **50**, 717-719.
- 14 H. Zhang and H. Cui, *Langmuir*, 2009, **25**, 2604-2612.
- 15 D. B. Zhao, Z. F. Fei, T. J. Geldbach, R. Scopelliti and P. J. Dyson, *J. Am. Chem. Soc.*, 2004, **126**, 15876-15882.
- 16 N. Kocharova, J. Leiro, J. Lukkari, M. Heinonen, T. Skala, F. Sutara, M. Skoda and M. Vondracek, *Langmuir*, 2008, **24**, 3235-3242.
- 17 B. Zhang, Y. Yuan, K. Philippot and N. Yan, *Catal. Sci. Technol.*, 2015, **5**, 1683-1692.
- 18 J. Dupont, G. S. Fonseca, A. P. Umpierre, P. F. P. Fichtner and S. R. Teixeira, *J. Am. Chem. Soc.*, 2002, **124**, 4228-4229.
- 19 A. Denicourt-Nowicki, B. Leger and A. Roucoux, *Phys. Chem. Chem. Phys.*, 2011, **13**, 13510-13517.
- 20 W. Zhu, Y. Yu, H. Yang, L. Hua, Y. Qiao, X. Zhao and Z. Hou, *Chem. Eur. J.*, 2013, **19**, 2059-2066.
- 21 E. Redel, J. Kramer, R. Thomann and C. Janiak, *J. Organomet. Chem.*, 2009, **694**, 1069-1075.
- 22 E. T. Silveira, A. P. Umpierre, L. M. Rossi, G. Machado, J. Morais, G. V. Soares, I. J. R. Baumvol, S. R. Teixeira, P. F. P. Fichtner and J. Dupont, *Chem. Eur. J.*, 2004, **10**, 3734-3740.
- 23 F. Jutz, J. M. Andanson and A. Baiker, *J. Catal.*, 2009, **268**, 356-366.
- 24 J. Julis, M. Hölscher and W. Leitner, *Green Chem.*, 2010, **12**, 1634-1639.
- 25 D. Gonzalez-Galvez, P. Lara, O. Rivada-Wheelaghan, S. Conejero, B. Chaudret, K. Philippot and P. W. N. M. van Leeuwen, *Catal. Sci. Technol.*, 2013, **3**, 99-105.
- 26 D. Zhu, H. Jiang, L. Zhang, X. Zheng, H. Fu, M. Yuan, H. Chen and R. Li, *ChemCatChem*, 2014, **6**, 2954-2960.
- 27 L. Zhang, X. Wang, Y. Xue, X. Zeng, H. Chen, R. Li and S. Wang, *Catal. Sci. Technol.*, 2014, **4**, 1939-1948.
- 28 Y. Sun, H. Fu, D. Zhang, R. Li, H. Chen and X. Li, *Catal. Commun.*, 2010, **12**, 188-192.
- 29 G. S. Fonseca, J. D. Scholten and J. Dupont, *Synlett*, 2004, 1525-1528.
- 30 V. Kogan, Z. Aizenshtat and R. Neumann, *New J. Chem.*, 2002, **26**, 272-274.
- 31 C. Chen, H. Chen and W. Cheng, *App. Catal. A*, 2003, **248**, 117-128.
- 32 H. Y. Jiang, C. F. Yang, C. Li, H. Y. Fu, H. Chen, R. X. Li and X. J. Li, *Angew. Chem., Int. Ed.*, 2008, **47**, 9240-9244.
- 33 H. Y. Jiang, B. Sun, X. X. Zheng and H. Chen, *App. Catal. A*, 2012, **421-422**, 86-90.
- 34 H. Y. Jiang and X. X. Zheng, *App. Catal. A*, 2015, <http://dx.doi.org/10.1016/j.apcata.2015.04.015>.
- 35 Z. F. Wu and H. Y. Jiang, *RSC Adv.*, 2015, **5**, 34622-34629.
- 36 R. A. Sheldon, M. Wallau, I. W. C. E. Arends and U. Schuchardt, *Acc. Chem. Res.*, 1998, **31**, 485-493.
- 37 T. Ohkuma, H. Ooka, T. Ikariya and R. Noyori, *J. Am. Chem. Soc.*, 1995, **117**, 2675-2676.
- 38 A. Perosa, P. Tundo and M. Selva, *J. Mol. Catal. A*, 2002, **180**, 169-175.
- 39 R. A. Sheldon, *Green Chem.*, 2005, **7**, 267-278.
- 40 L. Foppa and J. Dupont, *Chem. Soc. Rev.*, 2015, **44**, 1886-1897.
- 41 C. P. Mehnert, R. A. Cook, N. C. Dispenziere and E. J. Mozeleski, *Polyhedron*, 2004, **23**, 2679-2688.
- 42 S. Wesselbaum, U. Hintermair and W. Leitner, *Angew. Chem., Int. Ed.*, 2012, **51**, 8585-8588.